Polymer Testing 138 (2024) 108539

Contents lists available at ScienceDirect

Polymer Testing

journal homepage: www.elsevier.com/locate/polytest

# Mechanical reprocessing of polyurethane and phenolic foams to increase the sustainability of thermal insulation materials

Laura Simonini [a,b,*], Alessandro Sorze [a,b], Lorenza Maddalena [c], Federico Carosio [c], Andrea Dorigato [a,b]

[a] *Department of Industrial Engineering, University of Trento, Via Sommarive 9, 38123, Trento, Italy*
[b] *National Interuniversity Consortium of Materials Science and Technology (INSTM), Via Giusti 9, 50121, Florence, Italy*
[c] *Department of Applied Science and Technology, Politecnico di Torino-Alessandria Campus, Viale Teresa Michel 5, 10121, Alessandria, Italy*

ARTICLE INFO

*Keywords:*
Polyurethane
Phenolic resin
Foams
Mechanical recycling
Mechanical properties
Thermal conductivity

ABSTRACT

In this work polyurethane (PU) and phenolic foam (PF) panels were mechanically grinded and incorporated within an expanded polyurethane matrix utilized for thermal insulation, in order to reduce the use of virgin material and to promote a circular re-utilization of recycled materials. As observed by scanning electron microscopy, the formulations containing both recyclates showed a rather homogeneous cell structure, however their presence led to a strong reduction of the closed porosity. This reflected in a slight increase in the thermal conductivity, reaching maximum values of 0.030 W/m•K in foams with 7.5%wt of PF particles. The introduction of the recyclates slightly improved the thermal stability of the PU foams and led to a general decrease in flexural and compression properties. Cone calorimetry tests demonstrated that the inclusion of PF particles reduced the peak heat release rate up to 28 % compared to neat PU foam, enhancing the fire safety of the insulating panels.

## 1. Introduction

Nowadays the increasing interest in sustainable practices and environmentally friendly construction methods is affecting also the field of thermal insulation materials. These aspects involve the minimization of the heat transfer, the reduction of the energy consumption and the sustainable end of life management of the insulation panels [1–3]. In this scenario, polyurethane foams (PU) are widely recognized for their outstanding thermal insulating properties and have emerged as a preferred choice for insulating applications in several sectors, such as residential and commercial buildings, transportations and military industry [4–7]. PUs are low density thermosetting polymers that are synthesized from the exothermic reaction between polyols and polyisocyanates [8,9]. The intensification of their use has recently led to an increasing need of a more responsible end-of-life management, and recycling has been recognized as the most effective alternative to reduce their landfilling and increase their sustainability [10,11]. When PU foams contain at least 5 wt% by weight of recycled material, then they have the potential to significantly reduce the consumption of virgin resources and the environmental pollution associated to the production of the virgin panels. This threshold not only underscores the significance of incorporating recycled materials in foam production but also aligns with the objectives outlined in recent European legislative frameworks, aimed at promoting sustainability and circular economy principles within the manufacturing sector [12]. The recycling methods for polyurethanes are divided in mechanical recycling, chemical recycling, and energy recovery. Mechanical recycling involves the physical reprocessing of polyurethane waste to create new products or materials. PU waste is shredded and used as a filler or reinforcement in the production of new polyurethane products [13]. On the other hand, chemical recycling (such as through glycolysis and hydrolysis) breaks down the PU waste into its precursors or into other valuable chemicals for their reuse [14]. Conversely, energy recovery involves the incineration of the foam to generate heat and electricity. This last method does not directly recycle the PU into new products, but it helps to recover some of the embodied energy of the material [15]. Beside the beneficial effects associated to chemical recycling and energy recovery, the mechanical reprocessing still remains the most widespread practice due to its low cost, high efficiency and applicability to all kinds of foamed materials [16]. However, the main challenge of mechanical recycling is to maintain a regular cell structure of the foam even at elevated PU recyclate amounts, in order to avoid a loss of the thermal insulation properties in the resulting

---

* Corresponding author. Department of Industrial Engineering, University of Trento, via Sommarive 9, 38123, Trento, Italy.
*E-mail address:* laura.simonini@unitn.it (L. Simonini).

https://doi.org/10.1016/j.polymertesting.2024.108539
Received 30 April 2024; Received in revised form 19 July 2024; Accepted 5 August 2024

**Table 1**
Composition of polyol used in the present work.

| Constituent | CAS | Concentration (wt%) |
|---|---|---|
| **Aromatic polyesters** | 111-46-6 | 22.5 |
| **Halogenated polyetherpolyol B350** | 68441-62-3 | 22.5 |
| **Tris(2-chloro-1-methylethyl)phosphate** | 13674-84-5 | 22.5 |
| **Trans-1-chloro-3,3,3-trifluoropropene** | 102687-65-0 | 10.0 |
| **Triethylphosphate** | 78-40-0 | 3.0 |
| **Formic acid** | 64-18-6 | 1.5 |
| **N,N-Dimethylbenzylamine** | 103-83-3 | 0.5 |

foams. Therefore, one solution could be the incorporation of recycled insulation materials, having a higher insulating power, into the virgin polyurethane products, in order to compensate the negative effects on the cellular structure generated by the recyclate introduction. In this sense, phenolic foams (PF) can be considered as a valuable option. PFs are thermosetting polymers synthesized from the exothermic condensation between phenol and formaldehyde [17,18]. PFs are known for their excellent thermal insulation, fire resistance, limited smoke emission and high-temperature stability, which make them suitable for applications in fire-resistant construction systems [19,20]. However, PFs usually exhibit low compressive and flexural strength, high brittleness and high friability, which restrict their application fields [21]. As per PU, the continuous growth in their use must be counteracted by an improved recycling technology [22,23]. Mechanical recycling strategies for phenolic foams are nowadays focused on the optimization of the particle size distribution and the minimization of their thermal degradation during grinding and shredding operations [24].

Therefore, the aim of this work was to perform, for the first time, a comparative analysis of the potential of the mechanical recycling of PU and PF foams for the development of more eco-sustainable expanded polyurethane panels utilized in thermal insulation of the buildings. At this aim, commercial PU and PF foams were ground into two different particle sizes and incorporated within virgin PU foams at varying concentrations. By this process, it might be possible to reduce the use of virgin precursors and increase the recycled content in insulation panels. The resulting foamed materials were characterized from a morphological and thermo-mechanical point of view, with particular attention to their fire behavior.

## 2. Materials and methods

### 2.1. Materials

Polyol and diisocyanate, having viscosity of 1050 cPs and 200 cPs and density 1.10 g/cm$^3$ and 1.23 g/cm$^3$, respectively, were provided as liquids reagents by Kairos Srl (Verona, Italy) and used to prepare the virgin PU foam. The diisocyanate was fully constituted by diphenylmethanediisocyanate (MDI, CAS 9016-87-9100). Polyol was as a mixture of different substances, whose details are reported in Table 1. Recycled polyurethane foam was obtained by discarded panels (RBF312-C) having dimensions of 80 × 100 × 10 cm$^3$, supplied by Giona Holding Srl (Santa Maria di Zevio, Italy). These panels had a geometrical density equal to 0.040 g/cm$^3$ and a thermal conductivity of 0.022 W/m•K at 10 °C, as reported in the datasheet. Recycled phenolic foam was obtained by ISO FEN - VIT VV thermal insulating panels, with dimension of 60 × 120 × 10 cm$^3$, provided by Isolmec Group Spa (Como, Italy). This material had a geometrical density equal to 0.035 g/cm$^3$ and thermal conductivity of 0.019 W/m•K at 10 °C, as reported in the datasheet.

### 2.2. Sample preparation

Neat polyurethane foam was prepared by mixing at ambient temperature the liquid reagents, i.e., polyol and isocyanate, at a constant weight ratio of 100:130, as suggested by the supplier. The mixing process was performed at 300 rpm for 20 s to achieve a homogeneous mixture, that was then poured into a preheated (40 °C) mold having dimensions 250 × 250 × 25 mm$^3$, and placed in an oven for 20 min at 40 °C to obtain a foamed material. For the first 15 min a weight was positioned above the mold to prevent the formation of uneven panels, then it was removed to allow the material to relax for 5 min.

Recycled foams were prepared by grinding the discarded panels of PU and PF for 10 min by using an Ika Werke M20 mill (Ika AG, Staufer, Germany). The ground material was then sieved to recover granules having dimension ≤100 μm and 100–200 μm (respectively denoted with letter “f” and “c”, to indicate a fine and a coarse granulometry). The sieved material was dried at 40 °C overnight, then it was gradually added to the polyol and manually mixed for 20 s to achieve a homogeneous mixture. Isocyanate was then added to the mixture at the same relative weight ratio used for the production of neat PU foams, and stirred for additional 20 s. The mixture was then poured into the preheated mold (40 °C) and subjected to the foaming process previously described for neat PU panels. In this way, foams with a PF (or PU) recycled amount of 2.5 %wt, 5.0 %wt, and 7.5 %wt (with respect to the total weight of the liquid PU precursors) were prepared. These weight concentrations corresponded to a recycled PU content respectively equal to 40.1 %vol, 58.3 %vol and 68.3 %vol, and a recycled PF concentration respectively equal to 50.9 %vol 73.3 %vol and 85.9 %vol (with respect to the total volume of the liquid PU precursors). The recyclate volume concentrations with respect to the volume of the foams are equal to 5.4 %vol, 10.8 %vol and 16.2 %vol for the recycled PU, and to 6.2 %vol, 12.3 %vol and 18.5 %vol for the recycled PF. The denomination of the prepared samples is summarized in Table 2. In this manuscript, the sample nomenclature has been chosen to indicate the weight content of the recycled material.

**Table 2**
List of the prepared samples.

| sample | PU virgin (% wt) | Granulometry of recyclate (μm) | PU recyclate (% wt) | PF recyclate (% wt) | PU recyclate (% vol) | PF recyclate (% vol) |
|---|---|---|---|---|---|---|
| **PU** | 100.0 | – | – | – | – | – |
| **PF** | 0.0 | – | – | – | – | – |
| **PU2.5fPU** | 97.5 | ≤100 | 2.5 | – | 40.5 | – |
| **PU5fPU** | 95.0 | ≤100 | 5.0 | – | 58.3 | – |
| **PU7.5fPU** | 92.5 | ≤100 | 7.5 | – | 68.3 | – |
| **PU2.5cPU** | 97.5 | 100–200 | 2.5 | – | 40.5 | – |
| **PU5cPU** | 95.0 | 100–200 | 5.0 | – | 58.3 | – |
| **PU7.5cPU** | 92.5 | 100–200 | 7.5 | – | 68.3 | – |
| **PU2.5fPF** | 97.5 | ≤100 | – | 2.5 | – | 50.9 |
| **PU5fPF** | 95.0 | ≤100 | – | 5.0 | – | 73.3 |
| **PU7.5fPF** | 92.5 | ≤100 | – | 7.5 | – | 85.9 |
| **PU2.5cPF** | 97.5 | 100–200 | – | 2.5 | – | 50.9 |
| **PU5cPF** | 95.0 | 100–200 | – | 5.0 | – | 73.3 |
| **PU7.5cPF** | 92.5 | 100–200 | – | 7.5 | – | 85.9 |

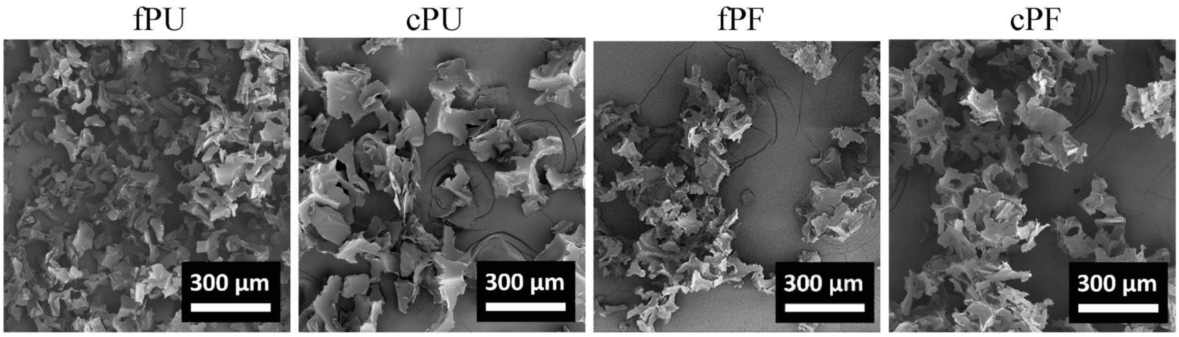

**Fig. 1.** SEM micrographs of recycled PU and PF particles.

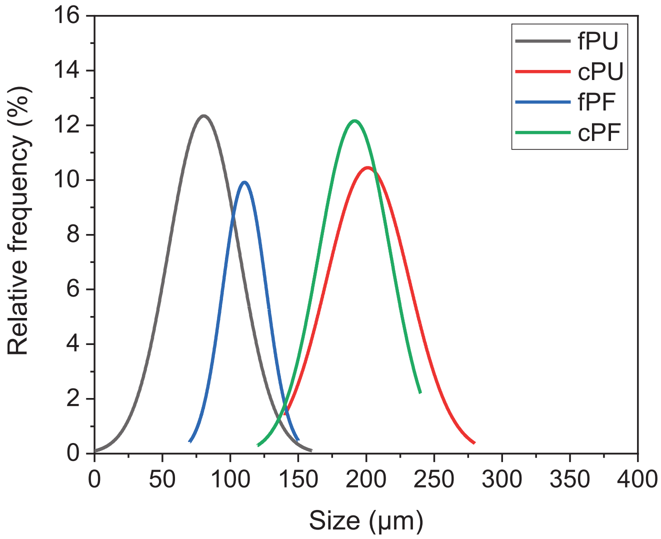

**Fig. 2.** Normal size distribution of recycled PU and PF particles after sieving.

**Table 3**
Mean size of recycled PU and PF particles after sieving.

| sample | size (μm) |
|---|---|
| **fPU** | 80.4 ± 25.8 |
| **cPU** | 201.2 ± 30.5 |
| **fPF** | 110.4 ± 16.1 |
| **cPF** | 191.5 ± 26.2 |

### 2.3. Experimental techniques

#### 2.3.1. Morphological analysis

The morphological appearance of the prepared foams was observed by field emission scanning electron microscopy (FESEM) using a Carl Zeiss AG-SUPRA 40 microscope (Carl Zeiss, Oberkochen, Germany) operating at an acceleration voltage of 3.5 kV. Before the observation, the samples were coated for 20 s with a thin Pt/Pd 80:20 coating to make them conductive, by using a Quorum Q150T ES sputter coater (Quorum Technologies, Lewes, UK).

The porosity of the foams was evaluated through the calculation of the geometrical and the theoretical density of the samples. The geometrical density ($\rho_{geom}$) is defined as the experimental density of a structure that includes defects and porosity, and it was calculated according to Equation (1):

$$\rho_{geom} = \frac{m_{sample}}{V_{geom}} \tag{1}$$

where $m_{sample}$ is the weight (in g) and $V_{geom}$ is the geometrical volume (in $cm^3$) of cylindrical samples, having radius of 12.5 mm and height of 25 mm, cut from the prepared foams. At least 5 specimens were measured for each composition. The theoretical density ($\rho_{th}$) is defined as the density of a structure without defects and porosity, and it can be obtained from the mixture rule (see Equation (2)):

$$\rho_{th} = \sum_{i=1}^{n} \varphi_i \bullet \rho_i \tag{2}$$

where $\varphi_i$ and $\rho_i$ are respectively volumetric fractions and the density of each constituent (i.e., polyol, isocyanate and PU/PF recycled foam). For polyol and isocyanate, the density at liquid state has been considered in the calculation, while for the PU/PF recyclate the density at foamed state, corresponding to the geometrical density reported in datasheet, has been taken into account. The apparent density ($\rho_{app}$) was measured with an Accupyc 1330 helium pycnometer (Micromeritics Instrument Corporation, Norcross, GA, USA) following ASTM D6226 standard. Measurements were conducted at a temperature of 23 °C, using a 1 $cm^3$ cell and performing 30 measurements for each sample. The total porosity ($P_{tot}$) was calculated as reported in Equation (3):

$$P_{tot} = \left(1 - \frac{\rho_{geom}}{\rho_{th}}\right) \tag{3}$$

The open porosity ($P_{open}$) was calculated as reported in Equation (4):

$$P_{open} = \left(1 - \frac{\rho_{geom}}{\rho_{app}}\right) \tag{4}$$

Therefore, the closed porosity ($P_{closed}$) was calculated as shown in Equation (5):

$$P_{closed} = P_{tot} - P_{open} \tag{5}$$

#### 2.3.2. Thermal properties

The thermal conductivity (λ) of the prepared foams was determined on specimens of 150 × 150 × 25 $mm^3$ using a Netzsch HFM 446 small lambda instrument (NETZSCH-Gerätebau, Selb, Germany) at constant temperature of 10 °C and according to ASTM C518-21. Three specimens were tested for each composition.

Thermogravimetric analysis on the prepared foams was conducted by using a Mettler TG50 machine (Mettler Toledo, Columbus, OH, USA) under a nitrogen flow of 100 ml/min and imposing a heating ramp from 30 °C to 700 °C and a heating a rate of 10 °C/min. The residual mass at 700 °C ($m_{700}$), the onset temperature of the degradation ($T_{onset}$) and the temperature of maximum degradation rate ($T_{max}$), obtained from the peak of the derivative of TGA thermogram (DTG), were assessed. Only one specimen was tested for each composition.

#### 2.3.3. Mechanical properties

Three-point bending tests were performed using an Instron 5969 machine (Instron® Mechanical Testing Systems, Norwood, MA, USA),

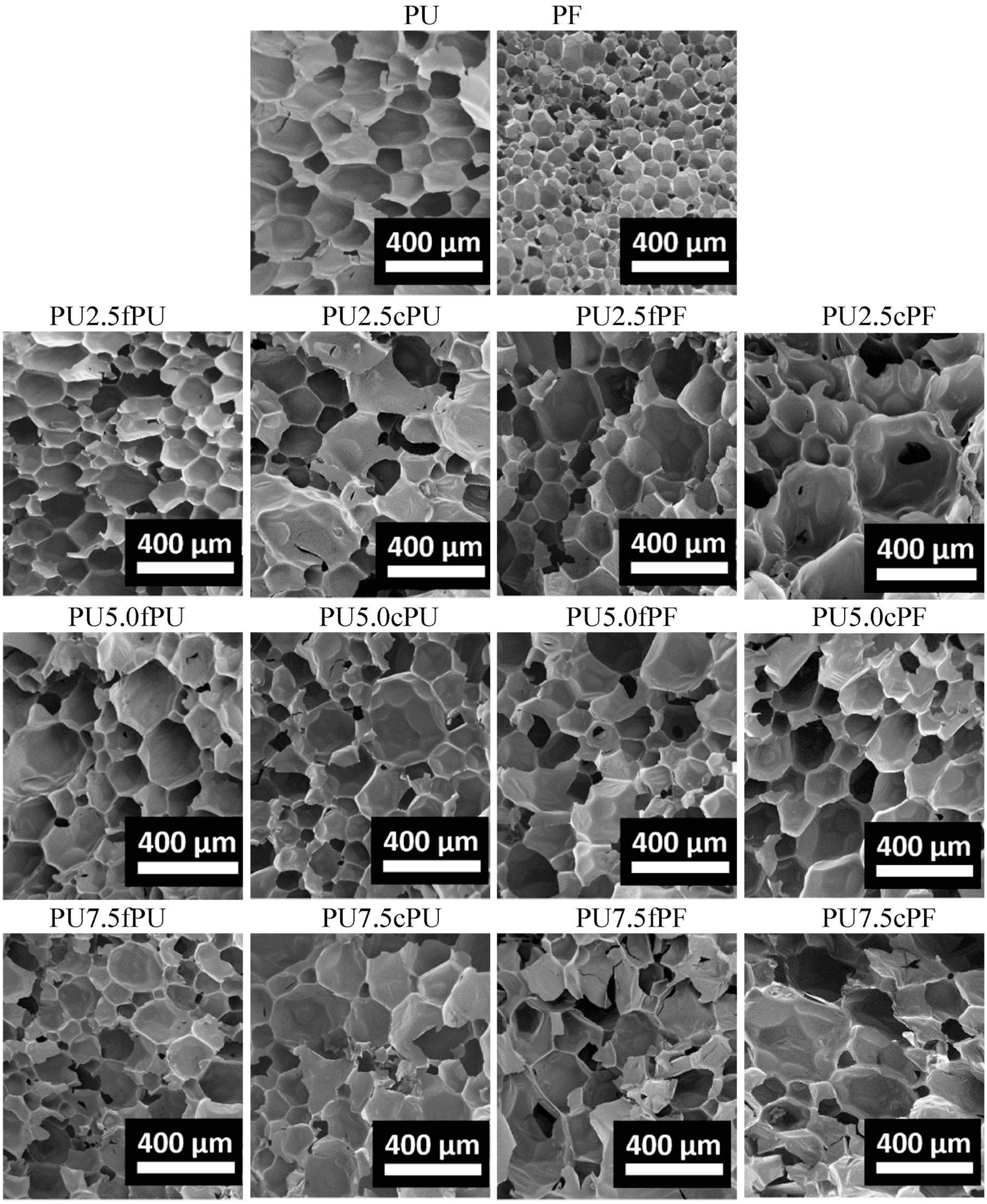

**Fig. 3.** SEM micrographs of the prepared foams.

equipped with a load cell of 1 kN, in order to determine the flexural modulus ($E_f$), the flexural strength ($\sigma_f$) and the flexural strain at break ($\varepsilon_f$) according to ISO 1209-2. The flexural properties were then normalized for the geometrical density of the foams. Samples had dimensions of 230 × 30 × 15 $mm^3$, and a span-to-depth ratio of 12 was used. The tests were carried out at constant temperature of 24 °C at a speed of 20 mm/min, and at least 10 specimens for each composition were tested.

Quasi-static compression tests were performed with the Instron 5969 machine (Instron® Mechanical Testing Systems, Norwood, MA, USA), equipped with a load cell of 1 kN, in order to determine the compressive modulus ($E_c$) and the compressive strength ($\sigma_c$), according to ASTM D1621-16 standard. Even in this case, the compressive properties were normalized for the geometrical density of the foams. Samples had dimensions 50 × 50 × 25 $mm^3$, tests were carried out at constant temperature of 24 °C, with a testing speed of 2 mm/min. At least 10 specimens for each composition were tested.

### 2.3.4. *Forced combustion tests*

Cone calorimetry measurements (Noselab, Milan, Italy) were conducted following ISO 5660-1 standard considering a 35 $kW/m^2$ radiative heat flux and setting a distance of 25 mm between the specimens and the

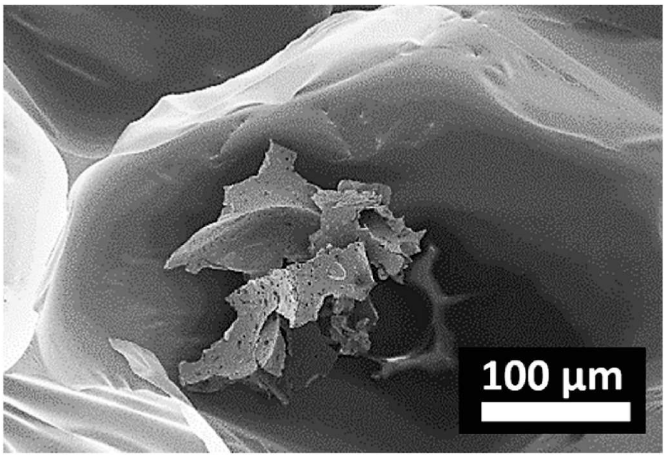

**Fig. 4.** SEM image showing the formation of an open pore due to the presence of a recycled PF particle within the virgin PU foam (sample PU7.5cPF).

radiation source. Specimens with dimensions 100 × 100 × 20 $mm^3$ were preliminarily conditioned at a temperature of 23 ± 0.1 °C and at a relative humidity of 50 ± 0.1 % for at least 48 h in climatic chamber, and all formulations were tested in triplicate. Post combustion cone calorimetry residues were analysed by a Zeiss Evo 15 scanning electron microscope (Carl Zeiss, Oberkochen, Germany) operating at 20 kV. Samples were positioned on conductive tapes and gold sputtered before the measurements.

## 3. Results and discussion

### 3.1. Morphological characterization

Representative SEM micrographs of the recycled PU and PF foams, after the sieving process, are reported in Fig. 1.

The sieved materials appear as sharp particles with irregular morphology. Their normal size distribution is shown in Fig. 2, while their mean dimension is numerically reported in Table 3.

The particles size reported in Table 3 corresponds to the dimensional ranges denoted as “fine” and “coarse” in Section 2.2. Their rather tight size distribution suggests that the materials have been efficiently ground and sieved, resulting in PU and PF foam recyclates with good morphological uniformity.

The cellular morphology of the prepared foams is shown in SEM micrographs displayed in Fig. 3.

Neat PU and PF foams show a regular cell structure with a uniform porosity and a clear definition of the cell walls. The mechanism of PU cell formation involves the reaction between isocyanate and polyol components, which leads to the generation of gaseous carbon dioxide that acts as a blowing agent, creating the cell structure. The presence of recyclates introduces nucleation sites, leading to the formation of smaller cells. Specifically, as observed from Fig. 3, the addition of the recycled foam particles allows to substantially maintain the regularity of the cell structure, but their presence is not clearly visible since they are embedded in the virgin PU foamed matrix. This suggests that, despite the elevated volume fraction of recyclate present in the liquid mixture, the PU precursors adequately wet the recycled particles, ensuring a rapid and efficient foaming process. On the other hand, the addition of PU and PF recyclates at a concentration of 7.5 %wt determines the most significant morphological changes in the cellular structure, from which a relative poor adhesion between matrix and filler can also be observed. Since the recycled powders used in this study come from fully foamed and crosslinked materials, they have already completely reacted and therefore have no chemical interactions with liquid PU precursors. Even if in these foams the homogeneity of the cellular structure is not dramatically impaired, the increased viscosity of the liquid matrix due to recyclate addition could have probably slowed down the crosslinking reaction within the PU matrix [25]. Moreover, from these micrographs it

**Table 4**
Mean pore size of the prepared foams obtained from normal size distribution.

| sample | size (µm) |
|---|---|
| **PU** | 188.5 ± 50.9 |
| **PF** | 62.9 ± 19.2 |
| **PU2.5fPU** | 117.4 ± 40.9 |
| **PU5.0fPU** | 155.6 ± 72.8 |
| **PU7.5fPU** | 101.4 ± 34.9 |
| **PU2.5cPU** | 153.7 ± 64.6 |
| **PU5.0cPU** | 116.7 ± 49.6 |
| **PU7.5cPU** | 134.9 ± 43.9 |
| **PU2.5fPF** | 145.1 ± 45.9 |
| **PU5.0fPF** | 135.6 ± 53.2 |
| **PU7.5fPF** | 123.4 ± 53.4 |
| **PU2.5cPF** | 182.4 ± 69.2 |
| **PU5.0cPF** | 144.3 ± 55.5 |
| **PU7.5cPF** | 143.2 ± 83.2 |

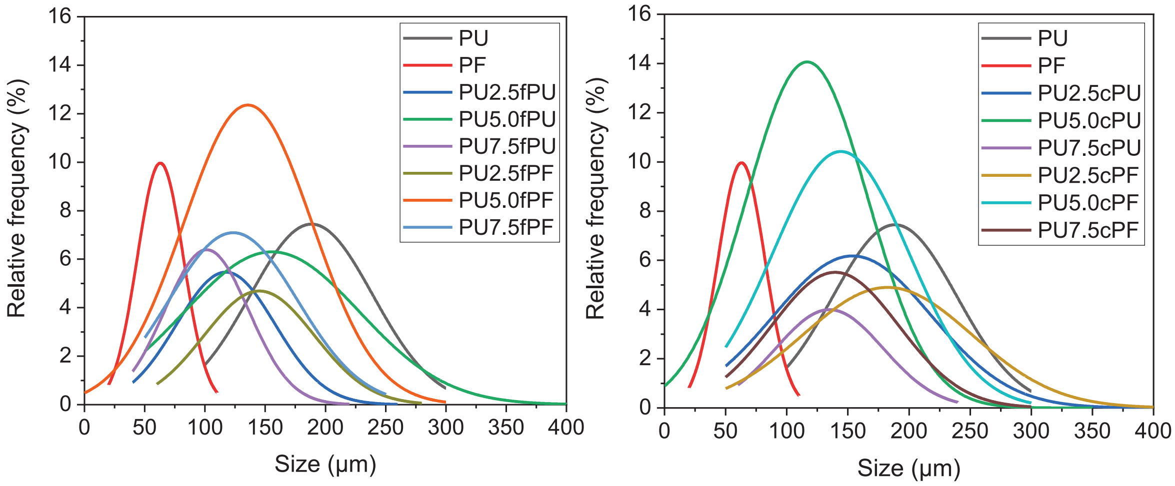

(a) (b)

**Fig. 5.** Normal distribution of the cell size of the foams prepared by using neat PU, neat PF and PU/PF recyclates with (a) fine and (b) coarse granulometry.

**Table 5**
Values of density and porosity of the prepared foams.

| sample | $\rho_{th}$ (g/cm$^3$) | $\rho_{geom}$ (g/cm$^3$) | $\rho_{app}$ (g/cm$^3$) | $P_{tot}$ (%) | $P_{closed}$ (%) |
|---|---|---|---|---|---|
| **PU** | 1.174 ± 0.003 | 0.044 ± 0.003 | 0.086 ± 0.009 | 96.3 ± 2.0 | 47.4 ± 2.0 |
| **PF** | – | 0.035 ± 0.003 | – | – | – |
| **PU2.5fPU** | 0.686 ± 0.004 | 0.057 ± 0.006 | 0.167 ± 0.002 | 92.1 ± 4.5 | 25.8 ± 2.5 |
| **PU5.0fPU** | 0.485 ± 0.003 | 0.062 ± 0.015 | 0.220 ± 0.007 | 87.5 ± 4.1 | 15.4 ± 0.2 |
| **PU7.5fPU** | 0.375 ± 0.012 | 0.059 ± 0.001 | 0.208 ± 0.013 | 84.0 ± 3.2 | 12.6 ± 1.5 |
| **PU2.5cPU** | 0.686 ± 0.004 | 0.049 ± 0.001 | 0.154 ± 0.007 | 92.2 ± 2.5 | 24.9 ± 1.1 |
| **PU5.0cPU** | 0.485 ± 0.003 | 0.048 ± 0.004 | 0.162 ± 0.010 | 90.1 ± 3.6 | 19.7 ± 1.1 |
| **PU7.5cPU** | 0.375 ± 0.012 | 0.058 ± 0.009 | 0.114 ± 0.040 | 85.7 ± 1.4 | 35.4 ± 1.1 |
| **PU2.5fPF** | 0.646 ± 0.011 | 0.055 ± 0.010 | 0.571 ± 0.024 | 92.3 ± 1.1 | 1.2 ± 1.1 |
| **PU5.0fPF** | 0.446 ± 0.007 | 0.048 ± 0.003 | 0.359 ± 0.013 | 89.3 ± 2.1 | 2.6 ± 0.2 |
| **PU7.5fPF** | 0.341 ± 0.003 | 0.050 ± 0.002 | 0.316 ± 0.008 | 87.1 ± 2.6 | 1.1 ± 0.2 |
| **PU2.5cPF** | 0.646 ± 0.011 | 0.052 ± 0.007 | 0.337 ± 0.026 | 92.6 ± 3.4 | 7.4 ± 0.1 |
| **PU5.0cPF** | 0.446 ± 0.007 | 0.055 ± 0.001 | 0.246 ± 0.002 | 88.9 ± 3.0 | 10.1 ± 0.1 |
| **PU7.5cPF** | 0.341 ± 0.003 | 0.059 ± 0.013 | 0.305 ± 0.039 | 93.6 ± 2.4 | 2.1 ± 1.5 |

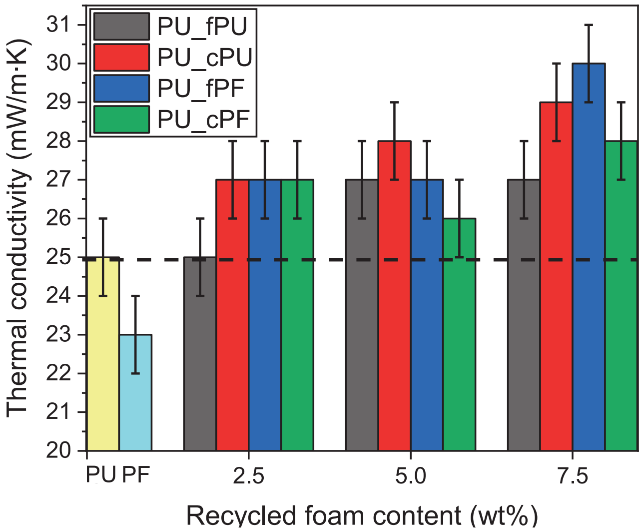

**Fig. 6.** Thermal conductivity values at 10 °C of the prepared foams.

is evident that some interconnected porosity is created in the foams upon the introduction of the recycled particles, and this could potentially affect their thermal conductivity. In particular, the brighter zones in the micrographs correspond to the closed pores, whereas the dark sections are related to the open holes. A clear visualization of this phenomenon can be seen in Fig. 4, where the presence of recycled PF particles induces the formation of open porosity in the foam structure.

The normal distribution of the cell size in the prepared foams is represented in Fig. 5(a and b), while the values of the mean cell size are numerically reported in Table 4.

The rather narrow distribution of cell size observed in all the prepared foams indicates that they are characterized by a quite homogeneous cellular structure. Neat PU foam has pores of 188.5 μm, while neat PF is characterized by a mean cell size of 62.9 μm. The lower pore size of PF foam could explain its lower thermal conductivity with respect to the neat PU sample. The introduction of the recycled foams considerably reduces the mean pore dimension, with a drop up to 46 % in the case of the PU7.5fPU sample. This could be related to the viscosity increase induced by the recyclate addition. However, there is not a clear trend related to the granulometry, the type and the concentration of the recycled foam added.

The values of theoretical density, geometrical density, apparent density, total and closed porosity are summarized in Table 5.

Neat PU foam exhibits a theoretical density of 1.174 g/cm$^3$. The introduction of both PU and PF recyclates, regardless of their granulometry, results in a reduction of the theoretical density. This is attributed to the partial replacement of the liquid precursors with a foamed filler, which has lower density values. Regarding the geometrical density, neat PU foam has density of 0.044 g/cm$^3$, and the addition of the recycled foam leads to a slight $\rho_{geom}$ increase, without a clear dependency on the concentration, type and size of recyclate. A similar observation can be performed analyzing the apparent density values: the neat PU foam shows a $\rho_{app}$ value of 0.086 g/cm$^3$, which increases upon the recyclate introduction. However, the addition of PF involves a stronger increase in $\rho_{app}$, which can be due to a higher tendency of PF particles to form open pores. Indeed, there is a correlation between the open porosity and the apparent density. Moreover, their high polarity can cause a partial agglomeration of the particles and renders more difficult the foaming process [17]. Consequently, also the total porosity results to be slightly affected by the presence of the recycled foam particles. In particular, the addition of recycled foam, regardless of the type and size, lead to a reduction of total porosity, from 96.3 % (neat PU) up to 84.0 % (PU7.5fPU). Neat PU shows 47.4 % of closed porosity, which is strongly reduced upon the recyclate addition due to the partial breakage of the cell walls. It is important to underline that a closed pores morphology is more suitable for thermal insulation application, while open porosity is desirable when elevated acoustic insulation properties are required [26]. The incorporation of recycled PU particles involves a reduction of closed porosity from 47.4 % up to 12.6 % (see PU7.5fPU sample), whereas the addition of PF particles results in a $P_{closed}$ reduction up to 1.1 % (see PU7.5fPF foam). In general, also for closed porosity, there is not a clear influence played by recycled PU and/or PF foam granulometry.

### 3.2. Thermal characterization

Fig. 6 shows the thermal conductivity (λ) values of the prepared foams at 10 °C.

Neat PU has a λ value equal to 0.025 W/m•K, while neat PF is characterized by a λ value equal to 0.023 W/m•K, and these values are slightly higher than those reported in the datasheet of the producer. This is probably due to the non-optimal conditions of the foaming process, that was performed by using a lab-made device. At a general level, the introduction of PU and PF recyclates leads to a slight increase of the λ values of the foams. This fact is probably related to the lower values of closed porosity and also to the slight decrease of the total porosity induced by the recycled foam addition. Nevertheless, considering also the standard deviation values associated to these results, it can be clearly seen that this increase is very low, especially up to a recyclate amount of 5 wt%. The most remarkable λ enhancement can be observed in the case of PU7.5fPF foam, where an increase of 16 % (0.030 W/m•K) compared to the neat PU foam can be registered. However, this value of thermal conductivity still remains within the λ range of the most common thermal insulating foams diffused on the market [27]. In particular, it is interesting to observe how the insulating capacity of the PU foams containing recycled PF particles is almost retained up to recyclate amount of 7.5 wt%, despite they experience a stronger reduction in the closed porosity. This suggests that the superior thermal insulation power of PF efficiently counteracts the $P_{closed}$ reduction due to recycled PF addition. There is not a distinct trend associated with the recyclate

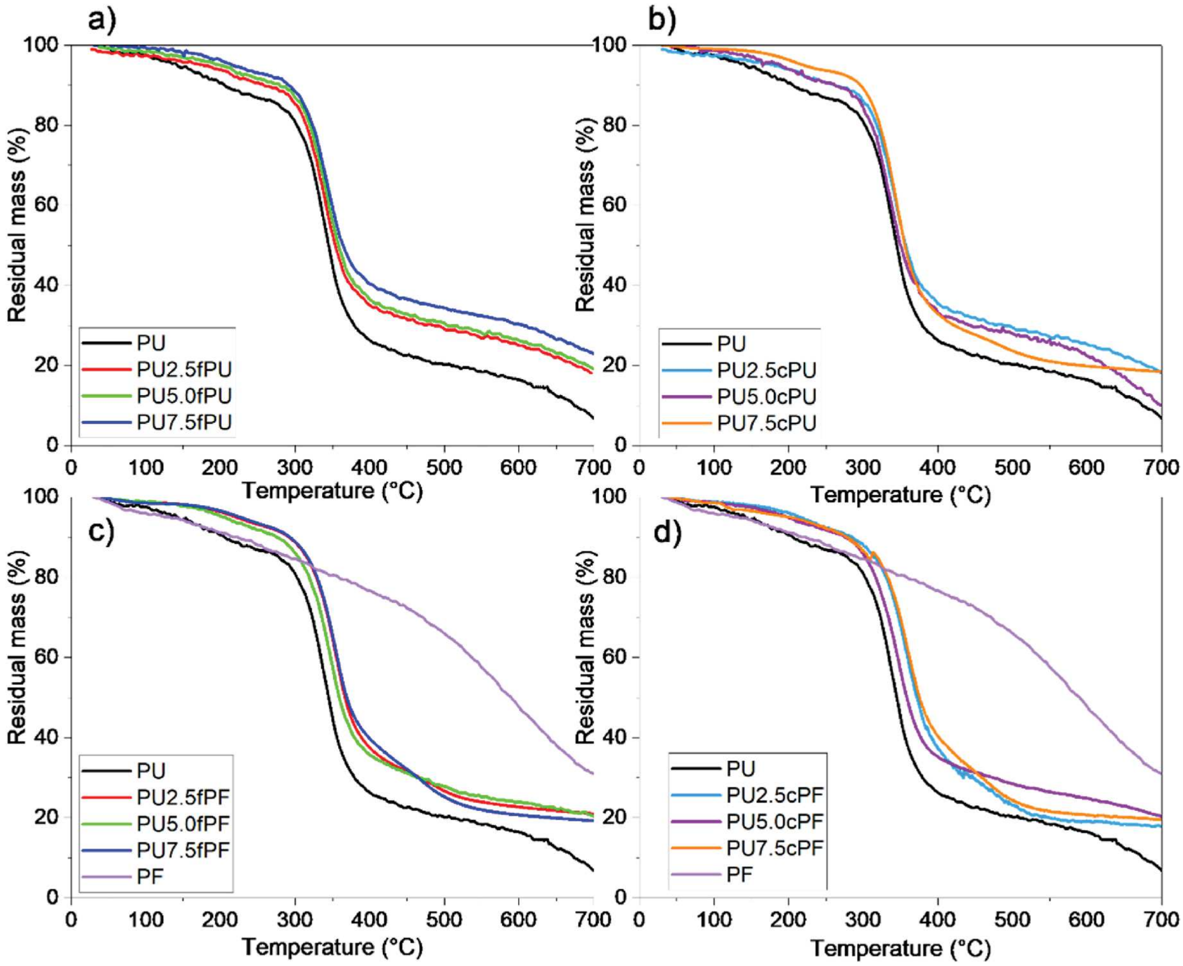

**Fig. 7.** TGA curves of neat PU, neat PF and foams with different contents of (a) fPU, (b) cPU, (c) fPF and (d) cPF recycled particles.

content up to 5 wt%, and the most promising results come from the PU2.5fPU and PU5.0cPF foams, which practically show the same λ values of neat PU. In general, there is no clear influence of the particle size of both PU and PF recyclates on the thermal conductivity of the foams.

In Fig. 7(a–d) and Fig. 8(a–d) the TGA and DTG curves obtained from thermogravimetric analysis on the prepared foams are respectively reported, while in Table 6 the most important results, expressed in terms of onset degradation temperature ($T_{onset}$), temperature of maximum degradation ($T_{max}$) and residual mass at 700 °C ($m_{700}$) are summarized.

The TGA thermogram of neat PU shows a residual mass of approximately 7 % at the end of the tests, while the incorporation of recycled PU and PF results in a further $m_{700}$ increase, without a clear correlation with the recyclate concentration. A similar amount of residual mass for PU foams is documented also in the literature [28]. The $T_{onset}$ of neat PU is 295 °C, while that of PF is equal to 470 °C. The introduction of recycled PU increases the $T_{onset}$ values up to 16 °C (see PU2.5cPU sample). However, variations in PU recyclate concentration and granulometry do not seem to significantly influence this increase. The introduction of PF further improves the $T_{onset}$ values, reaching 321 °C in the case of PU7.5cPF foam. Neat PU exhibits a $T_{max(PU)}$ of 336 °C, that is connected to the thermal decomposition of urethane bonds [28], and this value is substantially enhanced by the incorporation of PU recyclate, by reaching 355 °C in the case of the PU2.5cPU foam. This can be explained by the fact that the PU recyclate and the liquid precursors of the virgin PU foam come from different suppliers and, therefore, they could have a different chemical composition and/or flame retardant concentration (not specified by the supplier). On the other hand, the incorporation of PF has an even more positive impact on $T_{max(PU)}$ values, reaching 357 °C in the case of PU2.5cPF sample. This can be attributed to the fact that PF has a higher maximum degradation temperature ($T_{max(PF)}$) than PU, approximately at 597 °C, as also confirmed in literature [29]. In fact, the degradation of the PF constituent can be detected as a secondary peak in the DTG curves at approximately 480 °C. Also, for the maximum degradation temperatures there is no clear influence of the particle size of both recyclates. Therefore, from TGA tests it can be generally concluded that the introduction of both type of recyclates improves the thermal degradation stability of the resulting foams.

### 3.3. Mechanical characterization

In Fig. 9(a and b) representative stress-strain curves related to the flexural tests on the prepared foams are reported. In particular, Fig. 9(a) shows the flexural behavior of samples produced by using fPU and fPF recyclates, while in Fig. 9(b) the flexural properties of samples obtained introducing cPU and cPF recycled foams are shown.

In Table 7 the values of specific flexural strength, flexural modulus and flexural strain at break of samples are summarized, together with the deformation at break.

Neat PU foam behaves as a ductile material under flexural conditions, and it does not break in the strain interval considered. On the other hand, PF foam shows a brittle behavior, with a catastrophic failure at limited strain levels. Neat PU shows a specific flexural modulus of 216.4 MPa/(g/cm$^3$) and a specific flexural strength of 9.5 MPa/(g/cm$^3$), while neat PF has an $E_f/\rho$ value of 267.1 MPa/(g/cm$^3$) and a $\sigma_f/\rho$ of 10.0 MPa/(g/cm$^3$). The introduction of increasing amounts of fPU leads to a

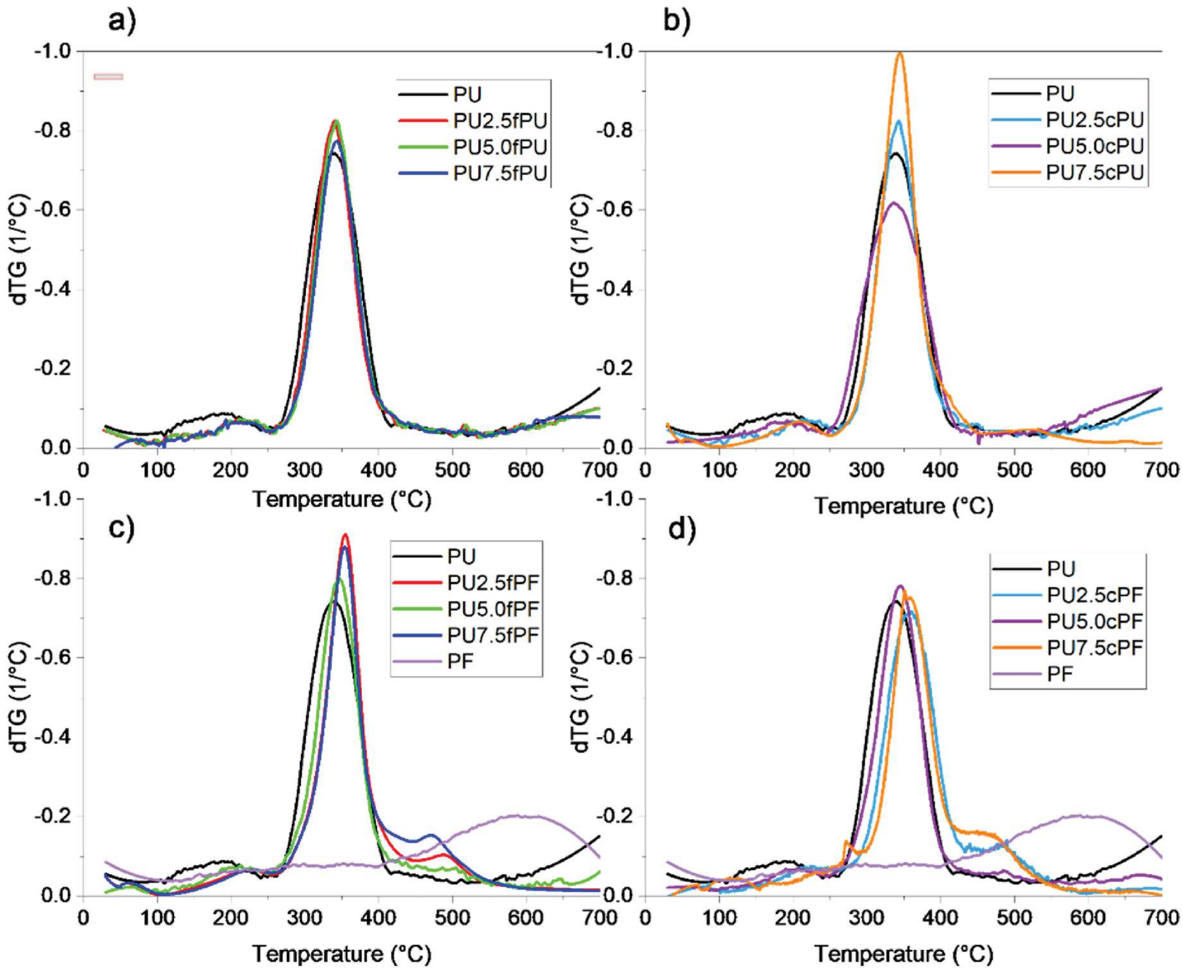

**Fig. 8.** DTG curves of neat PU, neat PF and foams with different contents of (a) fPU, (b) cPU, (c) fPF and (d) cPF recycled particles.

**Table 6**
Results of TGA tests on the prepared foams.

| Samples | $T_{onset}$ (°C) | $T_{max(PU)}$ (°C) | $T_{max(PF)}$ (°C) | $m_{700}$ (%) |
|---|---|---|---|---|
| **PU** | 295 | 336 | – | 6.8 |
| **PF** | 470 | 596 | 578 | 31.1 |
| **PU2.5fPU** | 297 | 339 | – | 19.0 |
| **PU5.0fPU** | 300 | 342 | – | 20.0 |
| **PU7.5fPU** | 304 | 343 | – | 23.0 |
| **PU2.5cPU** | 311 | 355 | – | 8.9 |
| **PU5.0cPU** | 293 | 340 | – | 10.0 |
| **PU7.5cPU** | 294 | 346 | – | 18.4 |
| **PU2.5fPF** | 295 | 354 | 487 | 23.1 |
| **PU5.0fPF** | 293 | 352 | 481 | 22.7 |
| **PU7.5fPF** | 300 | 353 | 498 | 19.9 |
| **PU2.5cPF** | 308 | 357 | 474 | 18.8 |
| **PU5.0cPF** | 301 | 352 | 481 | 20.2 |
| **PU7.5cPF** | 321 | 354 | 478 | 19.6 |

reduction in modulus and in strength (up to 28.7 % and 50.5 % for the PU5.0fPU sample, respectively), and to a general embrittlement, with a strong reduction of $\epsilon_f$ values. On the other hand, the addition of fPF has a stronger effect on flexural modulus and strength, with an even more evident degradation of both the properties. In fact, the flexural modulus of the PU7.5fPF foam is 157.2 MPa/(g/cm$^3$) (−27.4 % than PU) and the flexural strength is 3.0 MPa/(g/cm$^3$) (−68.4 % than PU). Regarding the samples containing recyclates with coarse granulometry, it can be noticed that the addition of 7.5 %wt of cPU and 7.5 %wt cPF leads to the reduction of the flexural modulus of 26.5 % and 36.4 %, respectively, and to a flexural strength drop of 36.8 % and 67.4 %, respectively. The observed decline in flexural properties may be attributed to several factors. Firstly, poor adhesion between the polyurethane matrix and the recyclates may lead to weak interfacial bonding, compromising the overall structural integrity of the foam. Additionally, a non-uniform distribution of the recyclates within the PU foam could result in localized areas of weakness, contributing to decreased flexural performance. Moreover, the presence of open porosity within the material increases its susceptibility to moisture absorption, which can further weaken the foam structure and negatively impact its flexural properties. This combination of factors underscores the importance of optimizing both material composition and processing parameters to enhance the mechanical performance of foams containing recycled materials.

In Fig. 10(a and b) representative stress-strain curves related to the compression tests on the prepared foams are reported. In particular, Fig. 10(a) shows the compressive behavior of samples produced by using fPU and fPF recyclates, while in Fig. 10(b) the compression properties of the foams obtained introducing cPU and cPF recycled foams are shown.

In Table 8 the results of compression tests, expressed in terms of specific compressive modulus and strength, are numerically summarized.

The introduction of increasing amounts of PU particles in fine granulometry leads to a slight reduction in the compressive modulus and a stronger reduction in compressive strength. In particular, neat PU shows compressive modulus of 75.9 MPa/(g/cm$^3$) and a compressive strength of 3.2 MPa/(g/cm$^3$), while PU7.5fPU sample has a compressive modulus of 55.3 MPa/(g/cm$^3$) (−27.1 % than PU) and compressive strength of 1.2 MPa/(g/cm$^3$) (−62.5 % than PU). On the other hand, the

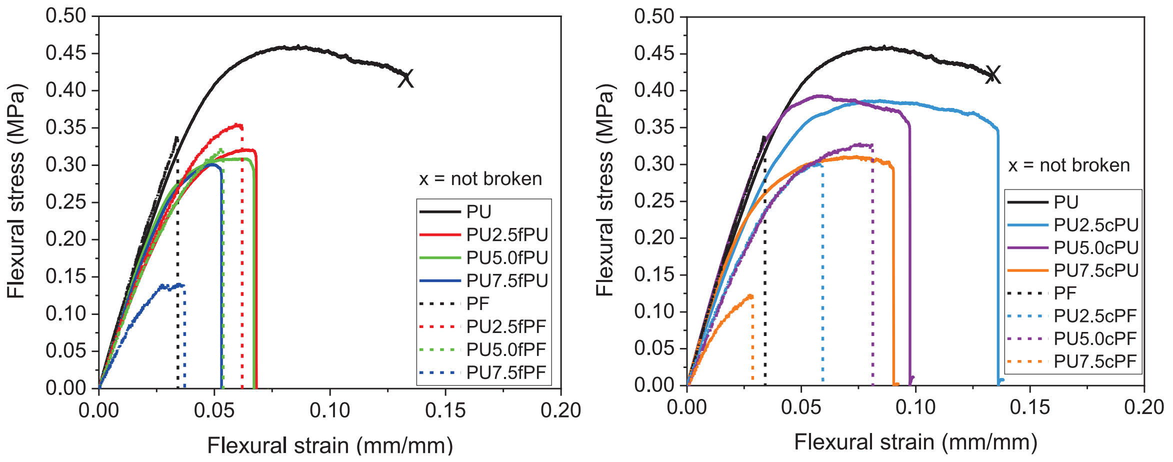

(a)                (b)

**Fig. 9.** Representative stress-strain curves from flexural tests on the prepared foams. Neat PU, neat PF and foams prepared with different amounts of (a) fPU and fPF, (b) cPU and cPF recyclates.

**Table 7**
Flexural properties of the prepared foams.

| Samples | $E_f/\rho$ (MPa/(g/cm$^3$)) | $\sigma_f/\rho$ (MPa/(g/cm$^3$)) | $\epsilon_f$ (mm/mm) |
|---|---|---|---|
| **PU** | 216.4 ± 22.7 | 9.5 ± 1.6 | – |
| **PF** | 267.1 ± 97.3 | 10.0 ± 3.1 | 0.03 ± 0.01 |
| **PU2.5fPU** | 148.9 ± 24.1 | 5.8 ± 0.8 | 0.07 ± 0.01 |
| **PU5.0fPU** | 154.5 ± 44.2 | 4.7 ± 1.5 | 0.07 ± 0.02 |
| **PU7.5fPU** | 162.0 ± 9.2 | 5.1 ± 0.6 | 0.05 ± 0.01 |
| **PU2.5cPU** | 192.0 ± 10.9 | 8.2 ± 1.8 | 0.15 ± 0.04 |
| **PU5.0cPU** | 189.8 ± 20.6 | 7.9 ± 0.9 | 0.11 ± 0.03 |
| **PU7.5cPU** | 159.1 ± 37.5 | 6.0 ± 2.1 | 0.10 ± 0.04 |
| **PU2.5fPF** | 150.4 ± 31.9 | 6.4 ± 1.9 | 0.07 ± 0.03 |
| **PU5.0fPF** | 182.3 ± 30.4 | 6.7 ± 0.8 | 0.05 ± 0.02 |
| **PU7.5fPF** | 157.2 ± 32.3 | 3.0 ± 0.3 | 0.04 ± 0.02 |
| **PU2.5cPF** | 158.8 ± 28.3 | 6.0 ± 1.2 | 0.07 ± 0.02 |
| **PU5.0cPF** | 169.3 ± 18.4 | 7.8 ± 1.4 | 0.09 ± 0.04 |
| **PU7.5cPF** | 137.6 ± 60.5 | 3.1 ± 1.7 | 0.06 ± 0.01 |

addition of fPF has a milder effect on the compressive strength and a stronger influence on the compressive modulus. In fact, by introducing 7.5%wt of fPF, the compressive strength results 2.8 MPa/(g/cm$^3$), but the modulus is reduced of about 24.4 %. The use of a recyclate with a coarser granulometry seems to have a stronger effect in the compressive properties than those exhibited in flexural mode. In fact, the

**Table 8**
Results of quasi-static compressive tests on the prepared foams.

| Samples | $E_c/\rho$ (MPa/(g/cm$^3$)) | $\sigma_c/\rho$ (MPa/(g/cm$^3$)) |
|---|---|---|
| **PU** | 75.9 ± 20.6 | 3.2 ± 0.7 |
| **PF** | 81.4 ± 20.1 | 4.3 ± 0.5 |
| **PU2.5fPU** | 59.6 ± 12.9 | 1.9 ± 0.9 |
| **PU5.0fPU** | 37.6 ± 18.2 | 1.5 ± 0.7 |
| **PU7.5fPU** | 55.3 ± 13.3 | 1.2 ± 0.5 |
| **PU2.5cPU** | 71.6 ± 6.2 | 2.7 ± 0.5 |
| **PU5.0cPU** | 54.6 ± 12.5 | 2.5 ± 0.6 |
| **PU7.5cPU** | 48.3 ± 23.2 | 1.0 ± 0.5 |
| **PU2.5fPF** | 51.8 ± 12.7 | 2.7 ± 0.9 |
| **PU5.0fPF** | 61.0 ± 5.5 | 2.7 ± 0.4 |
| **PU7.5fPF** | 57.4 ± 8.3 | 2.8 ± 0.7 |
| **PU2.5cPF** | 53.7 ± 9.7 | 2.1 ± 0.5 |
| **PU5.0cPF** | 36.4 ± 3.4 | 2.5 ± 0.6 |
| **PU7.5cPF** | 45.9 ± 15.7 | 2.9 ± 0.9 |

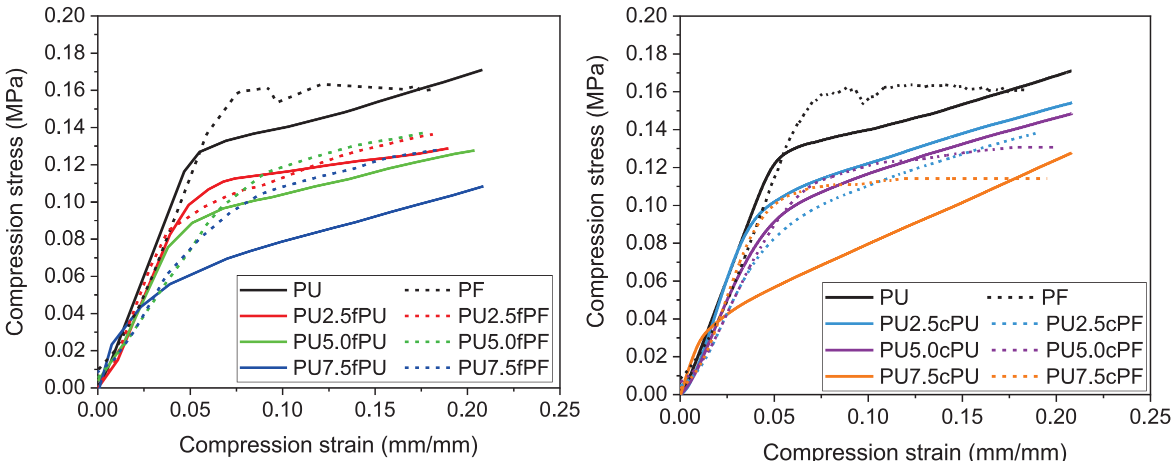

(a)                (b)

**Fig. 10.** Representative stress-strain curves from compression tests on the prepared foams. Neat PU, neat PF and foams prepared with different amounts of (a) fPU and fPF, (b) cPU and cPF recyclates.

**Table 9**
Comparative flexural and compressive properties from literature.

| | $E_f/\rho$ (MPa/(g/cm$^3$)) | $\sigma_f/\rho$ (MPa/(g/cm$^3$)) | $E_c/\rho$ (MPa/(g/cm$^3$)) | $\sigma_c/\rho$ (MPa/(g/cm$^3$)) |
|---|---|---|---|---|
| PU [22] | – | – | 6.5 ± n.d. | 198.4 ± n.d. |
| PU-5PPU [22] | – | – | 7.4 ± n.d. | 225.4 ± n.d. |
| PU [6] | 303.8 ± 27.8 | 13.6 ± 0.7 | – | – |
| PU-PCM20 [6] | 259.2 ± 10.3 | 10.6 ± 0.6 | – | – |

introduction of 7.5 %wt of cPU and cPF leads to a reduction of the compressive modulus of 36.4 % and 39.5 %, respectively, and to a drop of the compressive strength of 68.7 % and 9.3 %, respectively. Even in this case the observed decline in compressive properties can be attributed to the poor adhesion between the polyurethane matrix and recycled materials, to the uneven recyclate distribution and to the higher fraction of open porosity. In a future work a compatibilizing agent will be used to improve the interfacial interaction between the PU matrix and the recycled foams.

It is difficult to find in literature the mechanical performances of polyurethane systems similar to that investigated in this paper, therefore a direct comparison is rather difficult. However, Table 9 reports flexural

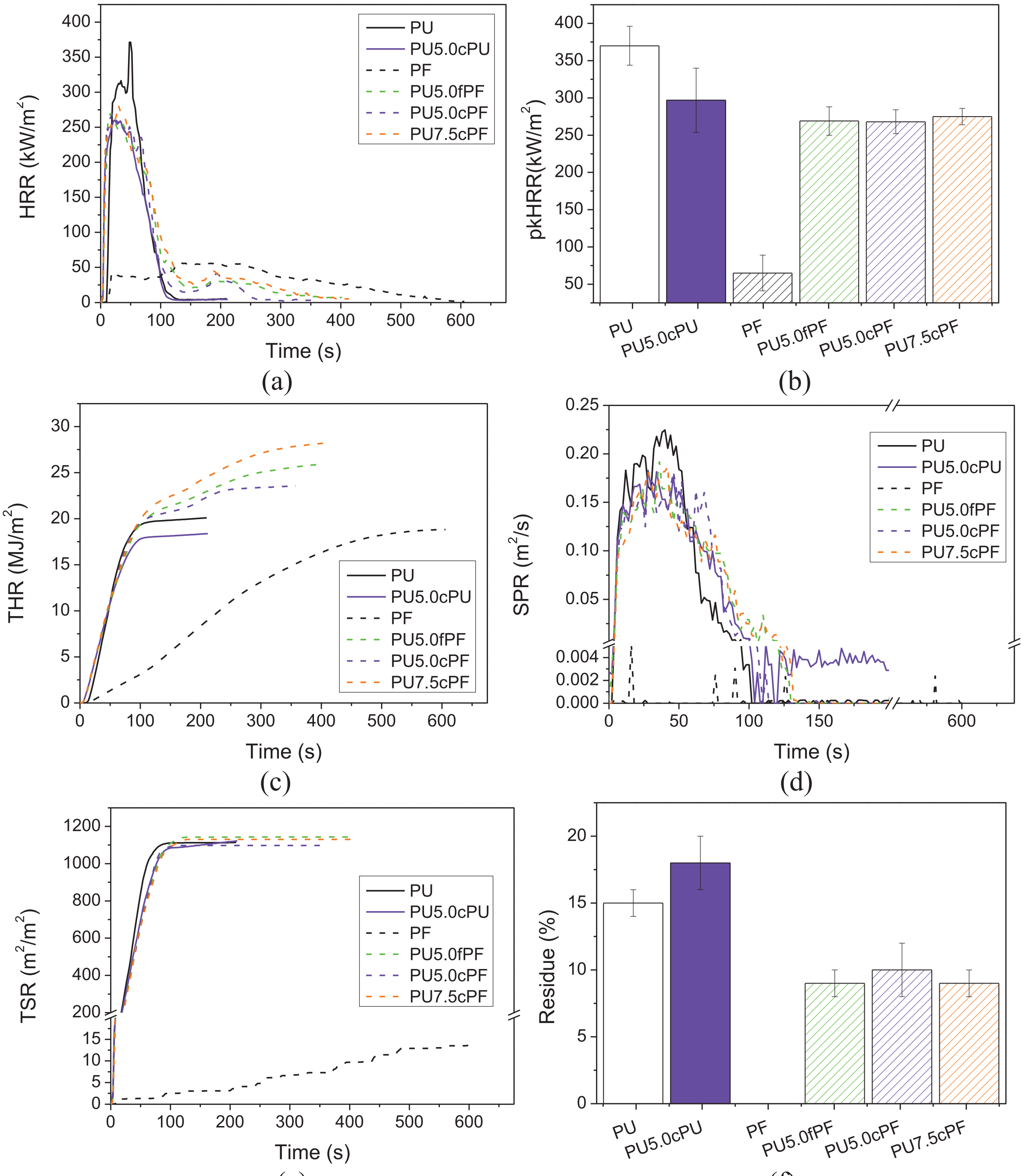

**Fig. 11.** Cone calorimetry tests on neat PU, neat PF and foams with optimized composition. (a) Heat release rate (HRR), (b) peak heat release rate (pkHRR), (c) total heat release (THR), (d) smoke production rate (SPR), (e) total smoke release (TSR), (f) residue at the end of cone calorimetry test.

**Table 10**

Results of cone calorimetry tests of neat PU, neat PF and the foams with optimized composition.

| Sample | TTI (s) | HRR ($kW/m^2$) | pkHRR ($kW/m^2$) | THR ($MJ/m^2$) | TSR ($m^2/m^2$) | Residue (%) |
|---|---|---|---|---|---|---|
| PU | 4 ± 1 | 96 ± 8 | 370 ± 26 | 20.0 ± 0.1 | 1160 ± 100 | 15 ± 1 |
| PF | 10 ± 2 | 29 ± 3 | 52 ± 6 | 19.1 ± 0.3 | 9 ± 4 | <1 |
| PU5.0cPU | 2 ± 1 | 91 ± 8 | 297 ± 43 | 19.3 ± 2.1 | 1164 ± 55 | 18 ± 2 |
| PU5.0fPF | 3 ± 1 | 70 ± 9 | 269 ± 19 | 25.8 ± 2.0 | 1141 ± 130 | 9 ± 1 |
| PU5.0cPF | 3 ± 1 | 68 ± 8 | 268 ± 16 | 25.0 ± 3.6 | 1163 ± 143 | 10 ± 2 |
| PU7.5cPF | 3 ± 1 | 71 ± 3 | 275 ± 11 | 26.4 ± 2.0 | 1121 ± 17 | 9 ± 1 |

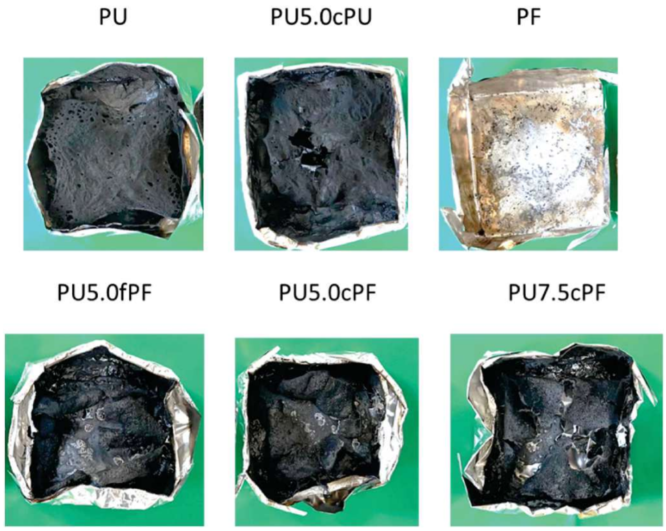

**Fig. 12.** Pictures of residues of the prepared foams after cone calorimetry tests.

and compressive properties of two PU in which 5 %wt of pulverized polyurethane particles with diameter ranging from 80 to 150 μm (PU-5PPU) and 20 %wt of microencapsulated phase change materials (PCM) with diameter 20 μm (PU-PCM20) were inserted. It can be noticed that the mechanical properties obtained in the present work are in line with these literature references, confirming thus the effectiveness of our experimental approach.

At the end of the morphological and thermo-mechanical characterization, the PU, PF, PU5.0cPU, PU5.0fPF, PU5.0cPF, PU7.5cPF were detected as the most promising ones, and their flame behavior was characterized through cone calorimetry tests.

### 3.4. Forced combustion tests

The aim of cone calorimetry measurements was to evaluate whether the inclusion of recycled PU and PF particles had a negative impact on the foam burning behavior. The tests have been performed under an irradiative heat flux of 35 $kW/m^2$, which is normally related to the early stages of a developing fire [30]. When exposed to the selected heat flux, the sample releases combustible volatiles that, upon reaching the flammability limits, lead to the flaming combustion of the specimen. The instrument then evaluates the heat release rate (HRR) and the smoke production rate (SPR) as a function of time. Fig. 11(a–f) reports the collected plots and integral values (THR and TSR for heat and fumes, respectively) as well as histograms related to the peak of heat release rate and final residue. Table 10 collects all the measured parameters.

Figs. 12 and 13 show pictures and SEM micrographs of residues of the same foams after cone calorimetry tests, respectively.

Upon exposure to the cone heat flux, the PU quickly ignites and burns with vigorous flames. The HRR plots steeply increases reaching a pkHRR at 370 ± 26 $kW/m^2$. During combustion, the foam structure is gradually consumed leaving a thin and dense charred residue, which accounts for 15 % of the original weight. By contrast, the neat PF shows extensive char formation that results in limited HRR values (pkHRR equal to 52 ± 6 $kW/m^2$) as well as reduced amount of smoke released. After the flame extinguishes, the charred residue is completely consumed by smoldering combustion (i.e., flameless combustion characterized by low HRR values). This behavior is a well-known characteristic of PF and extends the overall testing time [31,32].

As far as the samples containing recycled particles are concerned, the inclusion of cPU particles does not modify the burning behavior of the neat PU but produces a reduction in pkHRR (−20 %) and a slight increase in the final residue (+20 %). The other parameters remain mostly unchanged and within the experimental error. Similarly, during flaming combustion, the good char forming ability and low HRR of PF particles produces a substantial reduction in the pkHRR (up to −28 % for the PU5.0cPF foam). As the flame extinguishes, as already observed for the neat PF, the characteristic smoldering behavior of this latter is also displayed by the recycled foams. This is apparent from the low and prolonged HRR signal collected for samples PU5.0cPF, PU5.0fPF and PU7.5cPF after flame out. The smoldering duration seems to be directly related to the PF concentration. Interestingly, despite a different PF concentration, PU5.0fPF and PU7.5cPF show a similar behavior thus suggesting an effect of the granulometry where the higher surface exposed of the fine particles likely compensates for their reduced amount in the recycled foam with respect to the coarse ones. The occurrence of a smoldering combustion produces an increase in the THR and a subsequent reduction of the final residue. Smoke parameters remain unchanged with respect to the neat PU. The post combustion residues have been investigated by SEM (Fig. 13). The performed micrographs point out no substantial differences between the neat PU and the PU5.0cPU foams, highlighting the formation of a dense and compact char layer for both samples. Conversely, PF containing samples yield partially damaged structures characterized by holes that are likely ascribed to the observed smoldering behavior.

At a general level, it can be concluded that the inclusion of mechanically recycled foam particles in expanded PU panels results in a positive effect by reducing the pkHRR, that is often considered as one of the main fire safety parameters [33]. This can be ascribed to an improved char forming ability linked to the presence of PU and PF particles (as also observed by TGA, Fig. 7). Indeed, during combustion, the neat PU gradually collapses to a thin and dense charred structure that controls and partially limits the release of volatiles feeding the flame. The efficiency of such barrier is improved, to different extent, by the inclusion of PU and PF particles. Indeed, the PU5.0cPU sample yielded a rather compact and dense char layer that eventually achieved the highest wt% residue. Conversely, the superior char forming ability of PF particles only improved the char layer during flaming combustion as after flame out the residual char from PF was consumed by smoldering. This behavior produced small holes and defects within the residue (Fig. 13) and lead to an overall reduction of the final wt% residue.

### 3.5. General comparison of properties

A general comparison between the most important physical properties of the investigated foams is shown in Fig. 14 as radar plot. This comparative analysis has been performed in terms of thermal conductivity (λ), specific flexural modulus ($E_f/\rho$) and strength ($\sigma_f/\rho$), specific compression modulus ($E_c/\rho$) and strength ($\sigma_c/\rho$), and peak heat release rate (pkHRR).

From the radar plots it is evident the difference in properties between

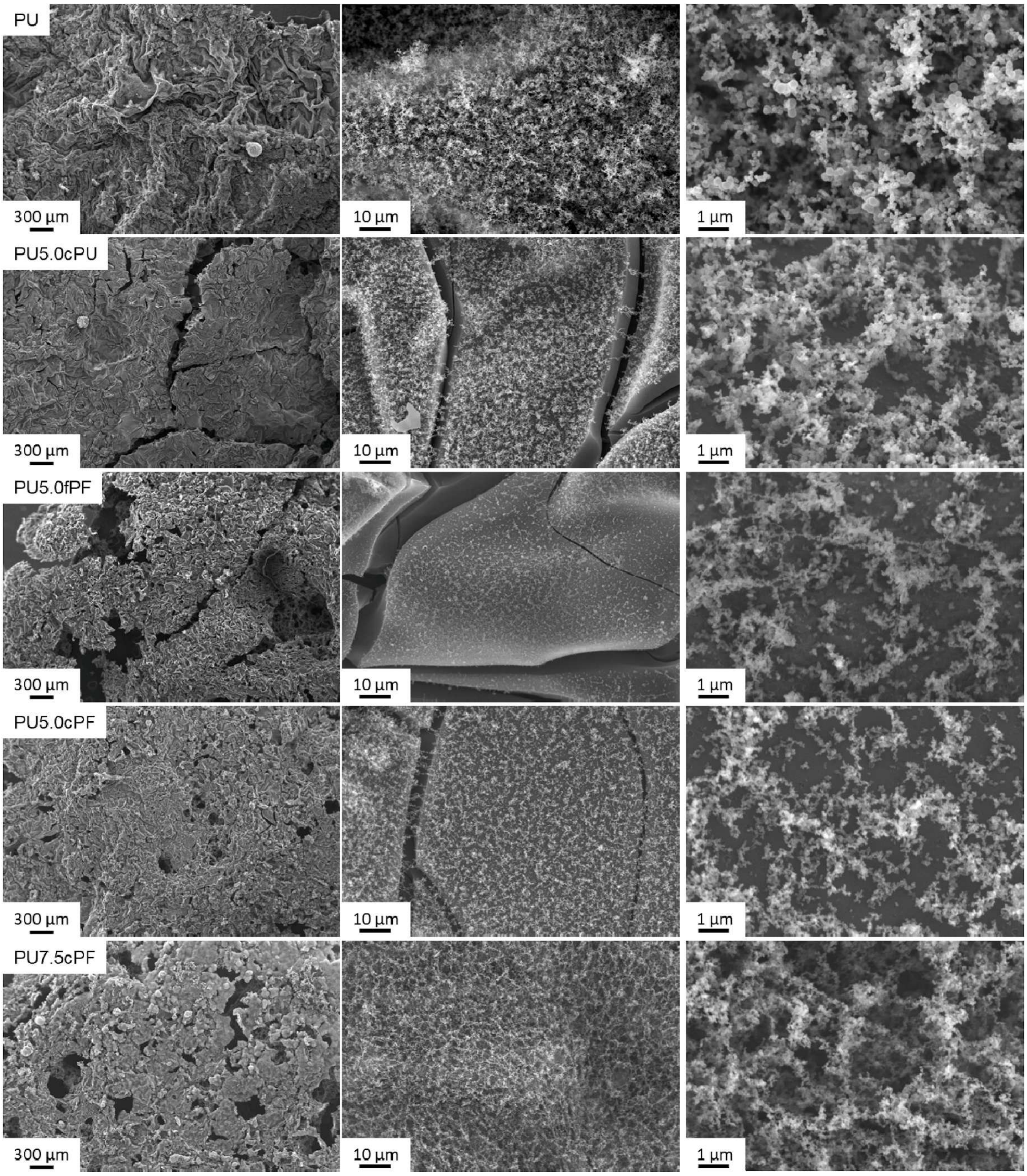

**Fig. 13.** SEM micrographs of residues of the prepared foams after cone calorimetry tests.

the samples that incorporate PU or PF recyclates compared to neat PU foam. PU foam shows a balanced distribution of properties from both mechanical and thermal point of view. However, its reaction to fire, expressed by the peak heat release rate (pkHRR), is significantly high, reaching a value of 370 ± 26 kW/m$^2$. This implies a higher heat release during combustion and faster burning, increasing the risk of fire spread. On the other hand, neat PF foam exhibits slightly superior mechanical properties, although the material is inherently more brittle compared to PU. Additionally, PF foam shows lower thermal conductivity than PU, making it more effective as a thermal insulator. The main advantage of PF foam is the significant decrease in pkHRR, which is around 52 ± 6 kW/m$^2$, compared to neat PU foam. This value is particularly important in terms of fire safety, as it indicates lower heat release and slower burning, thus reducing the risk of fire spread and providing more time for evacuation. However, it should be noted that the introduction of recycled foams compromises, albeit not drastically, the flexural and compressive properties. In particular, the foams with the highest PU and PF recyclate content show the greatest reduction in mechanical properties, especially under flexural conditions. On the other hand, the thermal conductivity is not substantially compromised by the addition of recycled foams. In the case of recycled PF particles, their higher thermal insulating performance counterbalances the negative effects played on the foam morphology. Among the samples tested, the most promising results emerge for the PU5.0fPF foam, as it highlights a suitable combination of mechanical strength, thermal insulating performance and fire behavior.

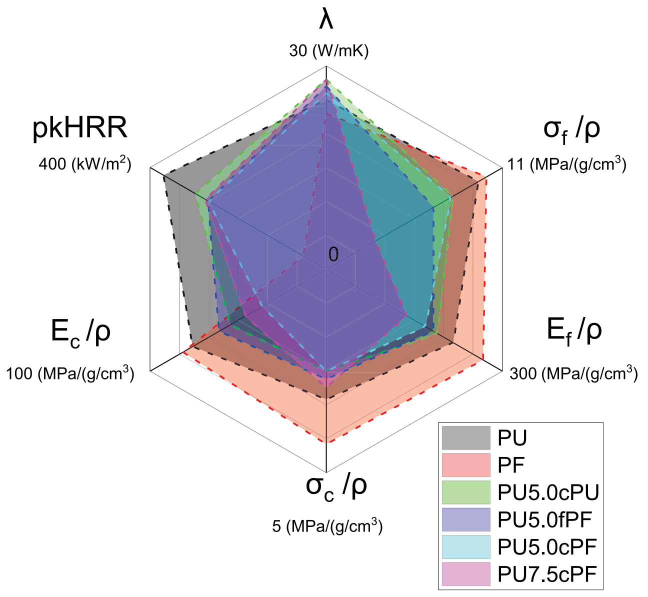

**Fig. 14.** Radar plot of the main physical properties of the investigated foams, specifically thermal conductivity (λ), specific flexural modulus ($E_f/\rho$) and strength ($\sigma_f/\rho$), specific compression modulus ($E_c/\rho$) and strength ($\sigma_c/\rho$), and peak heat release rate (pkHRR).

## 4. Conclusions

In this work discarded PU and PF panels were ground into two different particle sizes and incorporated at various amounts into expanded PU, in order to limit the consumption of virgin material and promote a novel circular economy approach for thermal insulating materials. The new formulations were characterized by a morphological and thermo-mechanical point of view. Field emission scanning electron microscopy revealed a consistent cell structure in the new formulations, due to an efficient wetting by the PU liquid precursors which allowed an effective foaming process. The incorporation of PU/PF recyclates led to a slight increase in foam density, thus resulting in a reduced closed porosity. This contributed to a slight enhancement in thermal conductivity, up to 16 % than neat PU with the highest fPF concentration, without dramatically comprosiming the thermal insulating power of these foams up to a recyclate amount of 5 %wt% Although the addition of PF/PU recyclate marginally improved the thermal stability, it adversely affected the flexural and compression properties of the foams, possibly because of the rather poor adhesion between virgin PU matrix and the recyclates and the higher degree open porosity. Nonetheless, according to cone calorimetry tests, the inclusion of recycled foams notably reduced the peak heat release rate by 28 % compared to neat PU, improving fire safety.

## Statements and declarations

No funding was received for conducting this study. The authors have no competing nor conflict of interest to declare that are relevant to the content of this article.

## CRediT authorship contribution statement

**Laura Simonini:** Writing – review & editing, Writing – original draft, Visualization, Validation, Software, Methodology, Investigation, Formal analysis, Data curation, Conceptualization. **Alessandro Sorze:** Writing – review & editing, Visualization, Validation, Software, Methodology, Investigation, Formal analysis, Conceptualization. **Lorenza Maddalena:** Writing – original draft, Visualization, Validation, Methodology, Data curation. **Federico Carosio:** Writing – review & editing, Visualization, Validation. **Andrea Dorigato:** Writing – review & editing, Visualization, Validation, Supervision, Conceptualization.

## Declaration of competing interest

The authors declare that they have no known competing financial interests or personal relationships that could have appeared to influence the work reported in this paper.

## Data availability

Data will be made available on request.

## Acknowledgments

The authors gratefully acknowledge Mr. Mattia Rizzi for the contribution carried out in the experimental part of the work.

## References

[1] B. Abu-Jdayil, A.H. Mourad, W. Hittini, M. Hassan, S. Hameedi, Traditional state-of-the-art and renewable thermal building insulation materials, Construct. Build. Mater. v214 (2019).
[2] M. Vasilache, M. Pruteanu, C. Avram, Use of waste materials for thermal insulation in buildings, Environmental Engineering and Management Journal v9 (2010).
[3] M. Massoudinejad, N. Amanidaz, R.M. Santos, R. Bakhshoodeh, Use of municipal, agricultural, industrial, construction and demolition waste in thermal and sound building insulation materials: a review article, Journal of Environmental Health Science and Engineering v17 (2019).
[4] N.V. Gama, A. Ferreira, A. Barros-Timmons, Polyurethane foams: past, present, and future, Materials v11 (2018).
[5] M. Ates, S. Karadag, A.A. Eker, B. Eker, Polyurethane foam materials and their industrial applications, Polym. Int. v71 (2022).
[6] F. Galvagnini, A. Dorigato, F. Valentini, V. Fiore, M. La Gennusa, A. Pegoretti, Multifunctional polyurethane foams with thermal energy storage/release capability, J. Therm. Anal. Calorim. v147 (2022).
[7] F. Galvagnini, F. Valentini, A. Dorigato, Development of polymeric insulating foams for low-temperature thermal energy storage applications, J. Appl. Polym. Sci. v139 (2022).
[8] F. Saint-Michel, L. Chazeau, J.Y. Cavaillé, E. C, Mechanical properties of high density polyurethane foams: I. Effect of the density, Compos. Sci. Technol. v66 (2006).
[9] H. Zhang, W.Z. Fang, Y.M. Li, W.Q. Tao, Experimental study of the thermal conductivity of polyurethane foams, Appl. Therm. Eng. v115 (2017).
[10] F. Quadrini, D. Bellisario, L. Santo, Recycling of thermoset polyurethane foams, Polym. Eng. Sci. v53 (2013).
[11] A. Magnin, L. Entzmann, A. Bazin, E. Pollet, L. Avérous, Green recycling process for polyurethane foams by a chem-biotech approach, Chemistry Europe v14 (2021).
[12] C. Pellegrino, F. Faleschini, C. Meyer, S. Mindess (Eds.), Developments in the Formulation and Reinforcement of Concrete, second ed., Woodhead Publishing, Cambridge, UK, 2019.
[13] A. Kemona, M. Piotrowska, Polyurethane recycling and disposal: methods and prospects, Polymers v12 (2020).
[14] Y. Deng, R. Dewil, L. Appels, R. Ansart, J. Baeyens, Q. Kang, Reviewing the thermo-chemical recycling of waste polyurethane foam, J. Environ. Manag. v278 (2021).
[15] J. Datta, M. Włoch, Recycling of Polyurethanes, Polyurethane Polymers, vol. 1, 2017.
[16] L. Zhang, S.C.Z. Liang, Influence of particle size and addition of recycling phenolic foam on mechanical and flame retardant properties of wood-phenolic composites, Construct. Build. Mater. v168 (2018).
[17] C. Mougel, T. Garnier, P. Cassagnau, N. Sintes-Zydowicz, Phenolic foams: a review of mechanical properties, fire resistance and new trends in phenol substitution, Polymer v164 (2019).
[18] S.A. Song, Y.S. Chung, S.S. Kim, The mechanical and thermal characteristics of phenolic foams reinforced with carbon nanoparticles, Compos. Sci. Technol. v103 (2014).
[19] P.R. Sarika, P. Nancarrow, A. Khansaheb, T. Ibrahim, Progress in bio-based phenolic foams: synthesis, properties, and applications, Chemical and Biomolecular Engineering v8 (2021).
[20] M.L. Auad, L. Zhao, H. Shen, S.R. Nutt, U. Sorathia, Flammability properties and mechanical performance of epoxy modified phenolic foams, J. Appl. Polym. Sci. v104 (2007).
[21] B. Del Saz-Orozco, M.V. Alonso, M. Oliet, J.C. Domínguez, F. Rodriguez, Mechanical, thermal and morphological characterization of cellulose fiber-reinforced phenolic foams, Compos. B Eng. v75 (2015).
[22] C. Yang, Z.H. Zhuang, Z.G. Yang, Pulverized polyurethane foam particles reinforced rigid polyurethane foam and phenolic foam, J. Appl. Polym. Sci. v131 (2014).

[23] R. Ebaid, Q. Wang, S. Faisal, L. Li, A. Abomohra, Valorization of floral foam waste via pyrolysis optimization for enhanced phenols recovery, Chemosphere v310 (2023).

[24] J. Liu, L. Wang, W. Zhang, Y. Han, Phenolic resin foam composites reinforced by acetylated poplar fiber with high mechanical properties, low pulverization ratio, and good thermal insulation and flame retardant performance, Materials v13 (2019).

[25] R. Beran, L. Zarybnicka, D. Machova, Recycling of rigid polyurethane foam: micro-milled powder used as active filler in polyurethane adhesives, J. Appl. Polym. Sci. v137 (2020).

[26] A. Drozdov, C. Claville, The effect of porosity on elastic moduli of polymer foams, J. Appl. Polym. Sci. v137 (2020).

[27] A.M. Papadopoulos, State of the art in thermal insulation materials and aims for future developments, Energy Build. v37 (2005).

[28] G. Trovati, E.A. Sanches, S.C. Neto, Y.P. Mascarenhas, G.O. Chierice, Characterization of polyurethane resins by FTIR, TGA, and XRD, J. Appl. Polym. Sci. v115 (2010).

[29] X. Sui, Z. Wang, Flame-retardant and mechanical properties of phenolic foams toughened with polyethylene glycol phosphates, Polym. Adv. Technol. v24 (2013).

[30] B. Schartel, T.R. Hull, Development of fire-retarded materials. Interpretation of cone calorimeter data, Fire Mater. v31 (2007).

[31] J.P. Hidalgo, J.L. Torero, S. Welch, Fire performance of charring closed-cell polymeric insulation materials: polyisocyanurate and phenolic foam, Fire Mater. v41 (2018).

[32] K. Tang, X. He, G. Xu, X. Tang, T. Ge, A. Zhang, Effect of formaldehyde to phenol molar ratio on combustion behavior of phenolic foam, Polym. Test. v111 (2022).

[33] V. Babrauskas, R.D. Peacock, Heat release rate: the single most important variable in fire hazard, Fire Saf. J. v18 (1992).